Rare Metal Materials and Engineering
Volume 51, Issue 7, July 2022
Available online at www.rmme.ac.cn

Science Press

Cite this article as: Li Zhishang, Xiong Zhihao, Yang Ping, et al. Simulation of Texture Evolution of Large TC18 Titanium Alloy Bar During Multi-pass Forging[J]. Rare Metal Materials and Engineering, 2022, 51(07): 2446-2453.

ARTICLE

Simulation of Texture Evolution of Large TC18 Titanium Alloy Bar During Multi-pass Forging

Li Zhishang[1], Xiong Zhihao[1], Yang Ping[1], Gu Xinfu[1], Yan Mengqi[2], Sha Aixue[2]

[1] School of Materials Science and Engineering, University of Science and Technology Beijing, Beijing 100083, China; [2] AECC Beijing Institute of Aeronautical Materials, Beijing 100095, China

Abstract: A multi-scale coupling method was used to predict the texture of TC18 titanium alloy bar. Firstly, the macroscopic finite element method was used to simulate the multi-pass forging process of TC18 titanium alloy bar under the conditions close to the actual ones, and the characteristics of inhomogeneous distribution of effective strain and shear stress σ_{XY} at the center and edge of the alloy bar during forging were obtained. Then, the multi-scale coupling method of macroscopic finite element model and mesoscopic visco-plastic self-consistent (VPSC) model was used to simulate the texture evolution at the center and edge of alloy bar during forging. The results show that in the center of the alloy bar, the texture transformation from {110}<112> to {111}<110> and from {110}<110> to {111}<110> occurs. The forging process is composed of mutual transformation between {111} and {110} textures. The transition texture shows the similar characteristics of shear texture in the pole figure. After analysis, it is confirmed that the transition texture is formed by the interaction of hexagonal forging and mutual transformation between {110} and {111} textures, which is not the shear texture. The {100} and {111} textures formed at edge were derived from the deformation process. Through comparison, it is found that the hexagonal forging can hardly produce the unfavorable {100} texture, and it is conducive to the weakening and elimination of {100} texture. The tensile test results show that the mechanical properties of the hexagonal forging specimen can meet the standard requirements.

Key words: titanium alloy; multi-pass forging; texture; simulation

TC18 alloy is a kind of $\alpha+\beta$ dual-phase titanium alloy with β phase transition temperature of 875 °C, high strength of 1080 MPa after annealing, and even higher strength of 1300 MPa after heat treatment[1]. Because of its high strength, good plasticity, low density, and good hardenability, TC18 alloy is widely used in aviation load-bearing structural parts.

However, TC18 titanium alloy also has many disadvantages, such as high deformation resistance, weak flow filling ability, and sensitivity to the deformation process parameters. TC18 alloy bars are usually forged by the multi-pass forging through the high temperature-low temperature-high temperature processes, which involves the single-phase and dual-phase region deformation[2]. According to the relationship between forging temperature and β phase transition temperature, the forging of titanium alloys can be divided into $\alpha+\beta$ forging and β forging[3]. Besides, the polygonal forging is also a common method to obtain the homogeneous microstructure through the repeated upsetting-stretching processes. Before the forge pieces are formed, the single-phase or dual-phase regions are pretreated by different forging processes to obtain different microstructures. Then, the forge pieces are formed and subsequently undergo the main forging process[4]. Before the main forging process, the dissipation efficiency distribution map is used to ameliorate the process parameters[5]. Because TC18 titanium alloy is very sensitive to the forging process, it is difficult to accurately control its evolution of microstructure and texture during hot working, on which the mechanical properties of titanium alloy mainly depend. Forging the large-sized titanium alloy bar can achieve the similar microstructures and textures for the produced relatively small bars along the axial, tangential, and radial directions from center to edge, thereby obtaining the similar mechanical properties. In general, during the forging at β phase region, almost all α phases are transformed into the β

Received date: July 18, 2021
Foundation item: National Science and Technology Project of China (JPPT-135-GH-2-017)
Corresponding author: Yang Ping, Ph. D., Professor, School of Materials Science and Engineering, University of Science and Technology Beijing, Beijing 100083, P. R. China, Tel: 0086-10-82376968, E-mail: yangp@mater.ustb.edu.cn

phases, and a typical basket structure is formed. During the forging at $\alpha+\beta$ phase region, α phases are usually equiaxed and elongated, and a typical dual-state structure is formed as a result of coexistence of dynamic recovery and recrystallization[6,7]. Although the volume fraction of β phase in TC18 titanium alloy is 70%~80% and 60% at 840 °C and room temperature, respectively, its mechanical properties are mainly affected by α phase morphology[8]. In general, during forging, the center of TC18 alloy bar is composed of lamellar primary α phase, and its edge consists of spherical primary α phase. The strength of lamellar primary $\alpha+\beta$ phase is slightly higher than that of the spherical $\alpha+\beta$ phase[7,9], but its plasticity and impact resistance are slightly lower than those of spherical $\alpha+\beta$ phase. In addition, the edge temperature is lower than center temperature during forging, resulting in obvious work hardening effect[10]. Therefore, the primary α phase morphology offsets the work hardening effect of β phase. Thus, different morphologies of α phase are not the main cause for the inhomogeneity of mechanical properties of alloy bar. Instead, the texture characteristics have an important effect on the mechanical properties of forged bars. The actual forging process of titanium alloy bar contains more than 10 passes, and the bars undergo the upsetting and stretching processes in each pass. Thus, the strong texture can be hindered and the near isotropy can be achieved for the forged bars. At present, the deformation texture of titanium alloy bars has been mainly investigated during the simple deformation process, such as uniaxial compression. Few reports show the texture evolution or formation prediction of titanium alloy bars in multi-pass forging process. It is found that the typical {100} and {111} textures are formed during the uniaxial compression of near-β titanium alloy[11-13]. Under the large deformation in single-phase region, the strong {100} texture is formed due to dynamic recrystallization[14]. If the strong <100> //bar axial texture exists at the bar center, the alloy strength will be reduced[15]. The formation and distribution of texture depend on the deformation conditions, and can seriously affect the mechanical properties of titanium alloys, such as tensile plasticity, crack nucleation, and fatigue life[16]. Therefore, the texture control is crucial to improve the mechanical properties of titanium alloys. Thus, a clear and accurate understanding of formation and evolution of texture in whole forging process is important to adjust the processing parameters in time and to finally obtain the satisfied alloy bars.

In recent years, with the rapid development of texture theory and computer technology, the prediction of texture evolution in forging process is more accurate. In order to obtain the formation and evolution of texture under actual forging conditions, a multi-scale coupling model was established in this study. According to the electron back-scattered diffraction (EBSD) analysis of TC18 titanium alloys under different conditions, it is found that TC18 titanium alloy cannot be fully statically recrystallized at near forging deformation rate, and the dynamic recrystallization only occurs at grain boundary to a small extent (deformation texture still occurs at relatively fast dynamic recrystallization rate). Therefore, the effect of recrystallization is not considered, and only the thermal deformation is considered.

1 Experiment

TC18 alloy with the nominal composition of Ti-5Al-5Mo-5V-1Cr-1Fe was used in this research. The forging bar with diameter of 300 mm was used in the forming process of large-sized TC18 titanium alloy bar. The bar was free-forged from original ingot through 20 MN rapid forging machine for more than 10 passes, and the last forming process was stretching. Free-forging process mainly included the upsetting and stretching. Fig. 1 shows the appearances of upsetting and stretching processes of large-sized TC18 titanium alloy bar during actual forging. In order to study the texture formation and evolution of TC18 titanium alloy bar during the whole forging process and each pass, the bar was cooled to room temperature in air after each pass, and the specimens for observation were taken from the center and edge of the cross section of alloy bars. The specimens were ground by 400#~3000# sandpaper, then electropolished with 5vol% perchloric acid alcohol solution under the conditions of 27.8 V and 60 s, and corroded by hydrofluoric acid immediately after polishing. Then, TESCAN VERA 3 LMH scanning electron microscope (SEM) equipped with EDAX DigiView5 high-resolution EBSD detector and OIM software was used to obtain the orientation distributions of specimens, and the maximum allowable deviation angle to typical texture was within 15°.

The multi-scale coupling method was used to simulate the forging process of TC18 titanium alloy bar by coupling macroscopic finite element model with mesoscopic visco-plastic self-consistent (VPSC) model[17,18]. At macroscopic scale, the cylindrical blank (Φ50 mm×100 mm), top die, and bottom die (120 mm×120 mm×30 mm) were established by Pro/E software firstly. Then, the finite element simulation software DEFORM was used to mesh the cylindrical blank, which was divided into 32 000 tetrahedral elements. The stress-strain curves under different deformation conditions were obtained by Gleeble thermal compression simulator, and the constitutive equation was obtained by numerical fitting. Different forging processes were simulated by changing the modeling parameters, such as deformation temperature, speed, and amount. The basic parameters of TC18 titanium alloy in the input software are shown in Table 1, and those used in

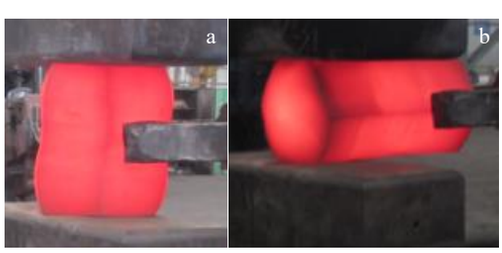

Fig.1 Appearances of upsetting (a) and stretching (b) processes of large-sized TC18 titanium alloy bar during actual forging

simulation process are shown in Table 2. DEFORM was used to simulate the macroscopic forging process of billet. After forging, the time increment and strain rate at different positions of bar were exported. At mesoscopic scale, the exported data from DEFORM were used as the input of mesoscopic model, and then VPSC was used to calculate the deformation texture of bar at different positions. The VPSC model assumes that the grains are ellipsoid and can be represented as a group of orientations. In addition, the grains are embedded in a homogeneous medium and subjected to homogeneous stress. VPSC model can deal with coordination of stress and strain between grains, and consider two deformation mechanisms of slip and twinning. The specific slip/twin systems and their related hardening parameters (τ_0, τ_1, θ_0, θ_1) were introduced in Ref. [19]. The total 500 grains were set, and one initial orientation was randomly assigned to each grain. The strain rate and time increment exported by macroscopic finite element model were used as input. With the continuous iteration of deformation calculation, the orientation of each grain changed constantly and was exported after specific time steps. Then, the texture evolution of TC18 titanium alloy during deformation was analyzed.

2 Results and Discussion

Because the actual forging process of TC18 titanium alloy bar is very complex and hard to simulate, the process was simplified on the basis of basic characteristics of forging process. Fig.2 shows the DEFORM simulation model of TC18 titanium alloy bar during forging process. The 1st pass of simulation process is similar to the 4th pass of actual forging. At 855 °C, the cylindrical blank was stretched with axial elongation of 30%, and then it was cooled to room temperature. The 2nd pass of simulation process is similar to the 5th pass of actual forging. At 930 °C, the cylindrical blank underwent upsetting with axial compression of 40% firstly, then was stretched with axial elongation of 40%, and finally was cooled to room temperature. The 3rd pass of simulation process is similar to the 7th (or 6th) pass of actual forging. At 843 °C, the cylindrical blank underwent upsetting with axial compression of 40% firstly, then was stretched with axial elongation of 40%, and finally was cooled to room temperature.

Fig. 3 shows the profiles of the effective strain distribution of alloy bar after each pass simulated by DEFORM. It can be seen that the effective strain at center of alloy bar is always higher than that at the edge of alloy bar after each pass, due to the large deformation zone in bar center and small deformation zone at bar edge. With the continuous forging process, the effective strain of bar is increased, and the difference between the effective strains in center and at edge is also increased. The initial difference between effective strains in center and at edge is 1.00, and the final difference is 1.69. Besides, the color in center is more homogeneous, indicating that the center deformation is more uniform; whereas the color of edge is not uniform with a color transition, indicating that edge deformation is uneven.

Although the main deformation modes in forging process of bar are upsetting and stretching, the alloy bar also suffers the shear stress at different positions, which has an effect on deformation and texture formation of bar at different positions. Fig. 4 shows the simulated profiles of the distributions of maximum shear stress σ_{XY} of alloy bar after each pass. It can be seen that after the 1st pass, there is a great difference in σ_{XY} between the center and edge of alloy bar, and the maximum shear stress σ_{XY} in center is smaller than that at edge. In the center of the alloy bar, σ_{XY} is small and negative; while at the edge of the alloy bar, σ_{XY} is large and positive. The maximum shear stress from the center to the edge of alloy bar gradually changes from negative to positive, which indicates that the stress at edge is much more complicated than that in center during the forging process. The maximum shear stress distribution in the alloy bar after the 2nd and the 3rd passes are basically consistent with that after the 1st pass. The only

Table 1 Basic parameters of TC18 titanium alloy

Density/g·cm^{-3}	Poisson's ratio	Emissivity	Elastic modulus/MPa	Coefficient of thermal expansion/m^2·s^{-1}	Specific heat/ J·(kg·°C)$^{-1}$	Burgers vector/m^{-1}
4.62	0.33	0.60	7450	2.2×10^{-5}	4.03	2.95×10^{-10}

Table 2 Basic parameters used in simulation

Billet temperature/°C	Mold temperature/°C	Friction coefficient	Mold movement speed/mm·s^{-1}	Thermal conductivity/W·m^{-2}·°C^{-1}
855~930	300	0.3	10	5

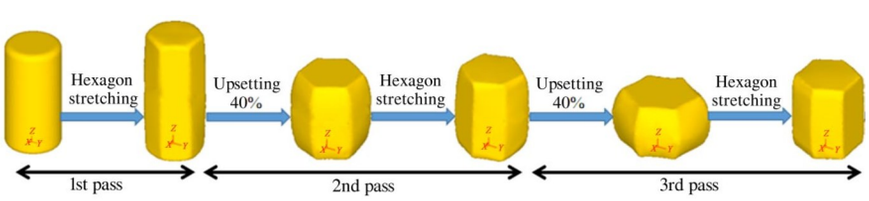

Fig.2 Simulation model of TC18 titanium alloy bar during forging process by DEFORM

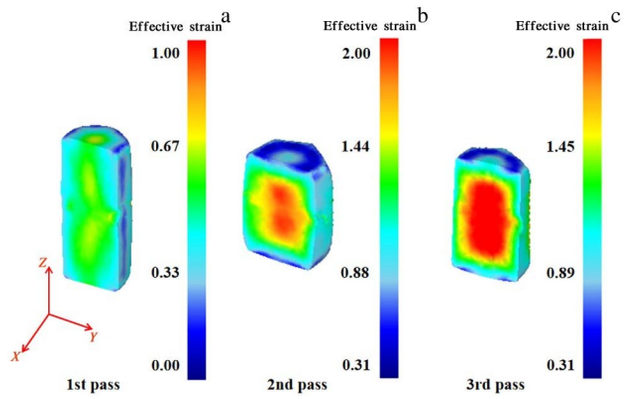

Fig.3 Simulated effective strain distributions of TC18 titanium alloy bar after the 1st pass (a), the 2nd pass (b), and the 3rd pass (c)

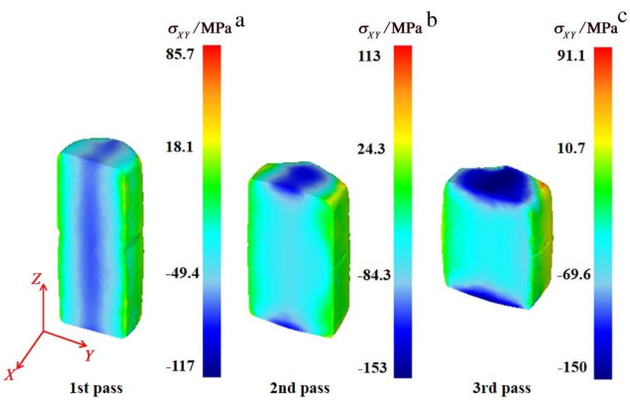

Fig.4 Simulated maximum shear stress (σ_{XY}) distributions of TC18 titanium alloy bar after the 1st pass (a), the 2nd pass (b), and the 3rd pass (c)

difference is that the distribution of the minimum value of maximum shear stress changes, which is originally parallel to *Z* axis through the center of alloy bar and is only distributed at the top and bottom ends of the alloy bar after the 2nd and the 3rd passes. In the positive center of alloy bar, σ_{XY} tends to be evenly distributed.

Through the analyses of distributions of effective strain and shear stress after each pass, it is found that the deformation and stress at the edge are more complex than those at the center during forging. The complex status at the edge, such as uneven deformation and large shear stress, has great influence on the formation and evolution of edge texture. In addition, the recrystallization and grain growth may occur when the alloy bar is reheated to high temperature after cooling for each pass, which will affect the initial texture of alloy bar for the next pass. Therefore, the specimens (3 mm×5 mm×10 mm) were taken from the center and edge of alloy bar after the 1st and the 2nd passes. Then, the specimens after the 1st and the 2nd passes were heated to 930 and 843 °C, respectively, and held for 5, 10, 15, and 60 min followed by quenching. The EBSD results of specimens after heat treatment were compared with those before heat treatment. It is found that the microstructure and texture of center specimens barely change, but the texture density decreases. The results show that the recrystallization occurs in edge specimens after heat treatment for 5 min. The texture tends to be random on the basis of original deformation texture, and {100} grains grow up with increasing the holding duration.

In order to define the texture obtained by simulation, the specimen coordinate system in DEFORM was defined as follows: *X* axis//rolling direction (RD), *Y* axis//tensile direction (TD), and *Z* axis//normal direction (ND). In simulation process, the initial texture has 500 random orientations. With the forging proceeding, the iterative calculation is conducted continuously, i.e., the texture formed in each pass is taken as the initial texture of next pass. For the center of alloy bar, the texture density is decreased when the alloy bar is reheated to the high temperature. Therefore, the texture density obtained after each pass is weakened by adding random orientations, and then the formed texture is used as the initial texture of next pass. For the edge of alloy bar, because the recrystallization is not considered in this model, the deformation texture after each pass is still used as the initial texture of next pass. The influence of recrystallization on edge texture was further investigated by comparing the simulation and experiment results.

Fig. 5 shows the orientation distribution function (ODF) diagrams at φ_2=45° calculated by VPSC to simulate the texture evolution during forging process. It can be seen that

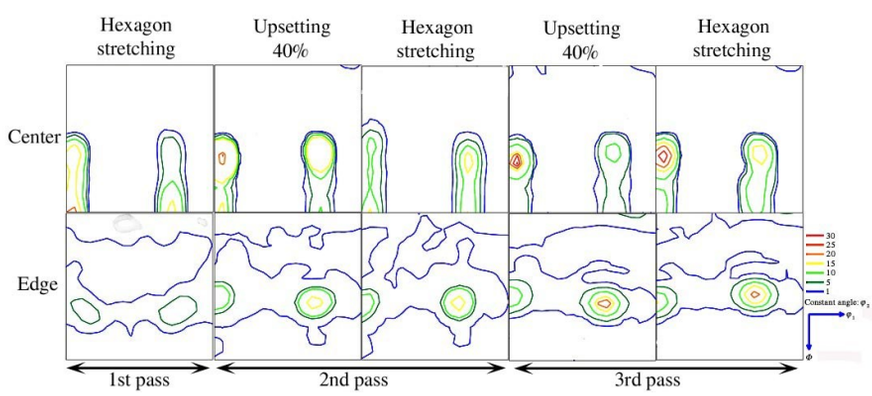

Fig.5 ODF diagrams at φ_2=45° calculated by VPSC for texture evolution simulation during forging process

after the 1st pass, {110}<112> and {110}<110> textures in center change to {111}<110> textures, while the weak {100} and {111} textures are formed at the edge. After the axial upsetting of 40% in the 2nd pass, the center texture remains unchanged, and it is still characterized by two transition textures. The density of {110}<112> and {110}<110> textures decreases significantly, while that of {111} <110> texture increases, indicating that {110} <112> and {110} <110> textures are transformed into {111} <110> texture after upsetting process. The {111} <110> edge texture are also enhanced with the existence of {100} texture. Then, after the hexagonal stretching, {111} <110> texture in the center of alloy bar changes to {110} texture, thereby enhancing the {110} texture with the transition texture characteristic; while there is no obvious change in the edge texture. After upsetting of 40% in the 3rd pass, the center texture does not change greatly, and the transition texture {110} is weakened. There is still no obvious change in edge texture, and {111} texture is enhanced. After hexagonal stretching, the transition texture {110} in the center is enhanced, while there is no transition texture in the edge of alloy bar. The strong {111} <110> texture and weak {100} texture exist in the edge of alloy bar. Generally, the {111} and {110} textures are mutually transformed in the center of alloy bar during the whole forging process, and the transition texture is formed, i. e., the stretching texture <110>//ND of body-centered cubic (bcc) structure is easily formed during the stretching, and the compression textures <111> and <100>//ND of bcc structure are easily formed during upsetting process. There is no obvious change in the edge texture, and the strong {111} texture and weak {100} texture exist all the time. The density of center texture is slightly higher than that of edge texture. The {100} texture is more likely to appear at the edge than at the center during forging.

The large-sized TC18 titanium alloy bars were directly air-cooled to room temperature after each pass, and then the specimens were taken from center and edge of forged bars. EBSD was conducted to detect the macroscopic texture characteristics of β phase. The average grain size is about 200 μm. The area measured at center and edge exceeds 4 mm×4 mm for each pass, and the number of grains is more than 100. Fig. 6 shows the grain orientation mapping measured at the center of alloy bar after the 1st pass. It can be seen that the distribution of grain size is not uniform, and there are orientation gradients in grains, which indicates the deformed grain state. Besides, the texture obtained is characterized by the deformation texture.

Because the 1st, 2nd, and 3rd passes of actual forging process are conducted under high temperature deformation, both dynamic recrystallization and static recrystallization occur. Thus, the texture is random and the simulation is meaningless. At present, the software cannot simulate the recrystallization process. Therefore, the three simulated forging processes in this research, the 1st, 2nd, and 3rd simulated process, correspond to the 4th, 5th, and 7th forging processes of the actual forging process, respectively (the 6th and 7th forging processes are the same). Thus, the textures of alloy bar after the 1st, 2nd, and 3rd simulation passes are compared with those after the 4th, 5th, and 7th passes during actual forging processes, respectively.

Fig.7 shows the {100}, {110}, and {111} pole figures of the simulated textures after the 1st pass and the measured textures after the 4th pass of forging at 855 °C. It can be seen that the simulation results of center textures are in good agreement with the measured ones. The textures are mainly {110} and {111} textures. Because of the transition between these two textures, the characteristics of shear texture can be observed in the pole figures. According to simulation results, the shear stress at the center of alloy bar during forging process is very small, which is mainly affected by the normal stress, and cannot form a strong shear texture. In addition, because the forging method is hexagonal forging, the texture characteristics of hexagonal forging can be observed, and the {110} and {111} textures are mutually transformed, leading to the connection between the two types of textures, as shown in Fig. 5 and Fig. 7a and 7c. Therefore, it is inferred that this texture is a transition texture formed by the interaction of hexagonal forging and mutual transformation of {110} and {111} textures, instead of a shear texture. The edge texture simulation results are also basically consistent with the measured ones. The edge texture contains {100} and {111} textures, and the texture characteristics of hexagonal forging can be observed in the pole figures. According to the previous results of effective strain distribution and shear stress distribution, the uneven strain distribution and large shear stress at the edge of alloy bar have a great influence on the

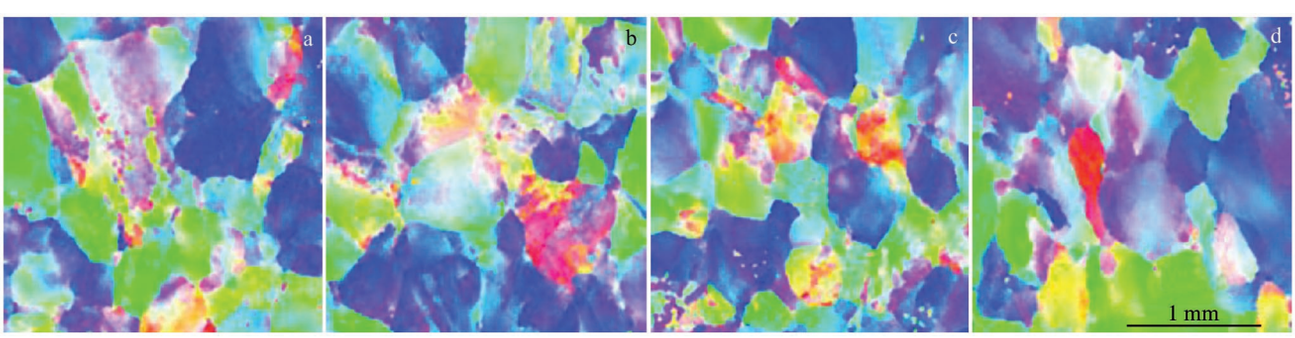

Fig.6 Grain orientation mappings measured in the center of TC18 titanium alloy bar after the 1st pass

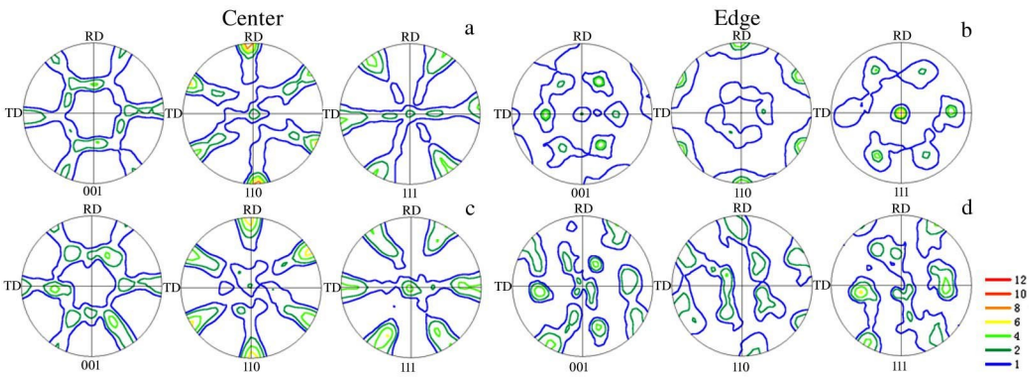

Fig.7 Pole figures of {100}, {110}, and {111} textures in the center (a, c) and edge (b, d) of TC18 titanium alloy bar after the 1st simulation pass (a, b) and the actual 4th pass of forging at 855 °C (c, d)

formation and evolution of edge texture. In addition, the recrystallization occurs at the edge of alloy bar when it is heated from room temperature to the forging temperature again, which randomizes the edge texture. Besides, although the forging of alloy bar has circumferential symmetry, the difference in forging sequence and deformation degree can also lead to different textures at different positions at the edge of alloy bar.

Fig. 8 shows the pole figures of {100}, {110}, and {111} textures after the 2nd simulation pass and the actual 5th pass of forging at 930 °C. It can be seen that the simulation results of center texture are in good agreement with the measured ones. After the 2nd simulation pass, the texture changes a little, but still shows the characteristics of hexagonal forging texture and transition texture. The {100} and {111} textures exist in both the simulation and experiment results of edge texture with some differences. The density of edge texture is lower than that of center texture, because the edge is a small deformation zone, and the relatively small deformation forms a weak texture. According to previous analysis, the {100} texture should be formed during the upsetting process, but it cannot be transformed into {110} texture in the later stretching process due to the small deformation of edge. Although this pass is forged in the single-phase region, the final texture is similar to the texture of the previous and following passes. The reason is that although the recrystallization occurs more easily during the single-phase forging at higher temperature than during the dual-phase forging at lower temperature, the dynamic recrystallization also occurs in forging process. After forging and cooling, the structure is still deformed, and the texture remains the characteristics of deformation texture.

Fig. 9 shows the pole figures of {100}, {110}, and {111} textures after the 3rd simulation pass and the actual 7th pass of forging at 843 °C. It can be seen that the simulation results of the center texture are in good agreement with the measured ones. The texture is basically the same as that of the previous passes, because the forging methods of each pass are basically the same. Thus, the texture is still characterized by the hexagonal forging texture and transition texture. The simulated edge texture is basically the same as that from the experiment results. The measured texture is more random due to the recrystallization. However, it can be seen that the measured edge texture still retains the basic characteristics of deformation texture. The transition texture does not form throughout the edge. According to ODF diagrams of simulated edge texture in Fig. 5, it can be seen that there are always {100} and {111} textures at the edge of alloy bar, and there is

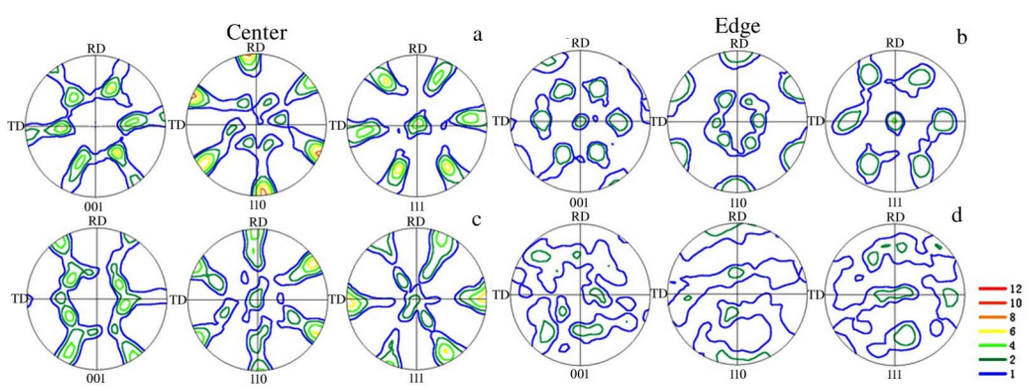

Fig.8 Pole figures of {100}, {110}, and {111} textures in the center (a, c) and edge (b, d) of TC18 titanium alloy bar after the 2nd simulation pass (a, b) and the actual 5th pass of forging at 930 °C (c, d)

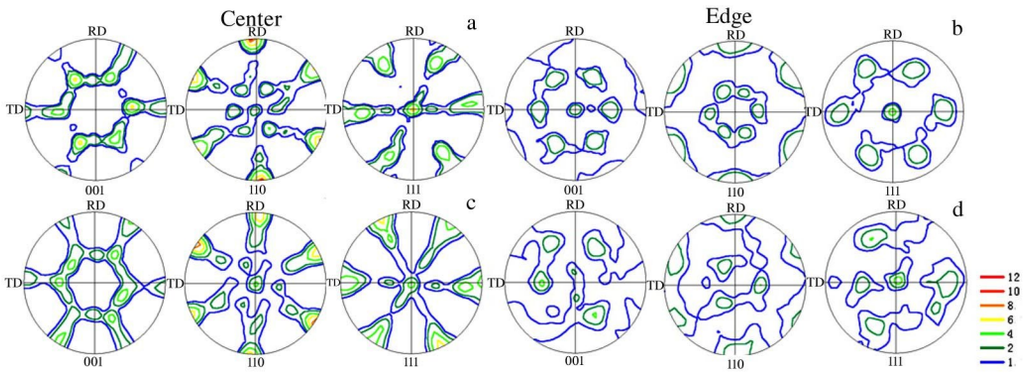

Fig.9 Pole figures of {100}, {110}, and {111} textures in the center (a, c) and edge (b, d) of TC18 titanium alloy bar after the 3rd simulation pass (a, b) and the actual 7th pass of forging at 843 °C (c, d)

no transition among {100}, {111}, and {110} textures. In addition, there is no connection between {100} and {111} textures in the pole figures, only presenting the texture characteristics of hexagonal forging. Therefore, the center texture is not the shear texture, and it is formed by the interaction of hexagonal forging and mutual transformation between {111} and {110} textures. There is always a weak {100} texture in the simulated and measured textures at the edge of alloy bar. Besides, the weak {100} texture in the alloy bar after actual forging is derived from the deformation process.

This research further investigated the texture evolution on the basis of the results in Ref.[19,20]. Firstly, in this research, the simulated forging process is much closer to the actual forging process, and the simulation results are directly compared with the actual production results of forging bar, showing the prediction accuracy. Secondly, the area of texture measurement is enlarged to increase the statistical data for precious simulation. Thirdly, the hexagonal forging is used in this research instead of square forging. By comparing the textures formed by these two methods, it is found that the square multi-directional forging can easily form the unfavorable strong {100} texture in the alloy bar; instead, the hexagonal forging can weaken the {100} texture formed by recrystallization. This result is of great significance for elimination or decrease of unfavorable {100} texture in the actual production. In fact, the <110> and <111> oriented grains are hard-oriented grains, while the <100> oriented grains are soft-oriented grains. Therefore, {110} and {111} textures are expected, whereas the {100} texture is unfavorable in the actual production and only appears at the edge of alloy bar, which is different from the results in Ref.[10].

In order to obtain the actual mechanical properties, the tensile tests were conducted along the axial (Z) direction of alloy bar at the center and edge according to GB/T 228-2002. The size of tensile specimen is shown in Fig.10. For the center of alloy bar, the yield strength $\sigma_{p0.2}$=1096 MPa, tensile strength σ_m=1134 MPa, elongation A=17.3%, and the shrinkage of the section Z=48.3%. For the edge of the alloy bar, $\sigma_{p0.2}$=1109 MPa, σ_m=1125 MPa, A=15%, and Z=49.3%. It can be seen that

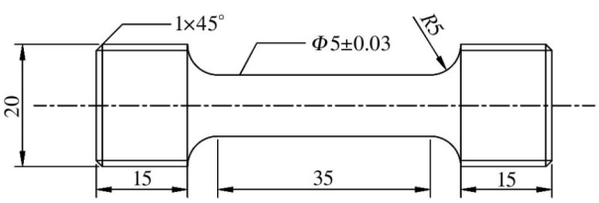

Fig.10 Schematic diagram of tensile specimen

the test results are much higher than the standard values ($\sigma_{p0.2}$= 1010 MPa, σ_m=1080~1280 MPa, A=8%, Z=20%). Therefore, this research shows a possible way to avoid the formation of unfavorable {100} texture and to improve the mechanical properties of TC18 titanium alloy bar.

In this research, the macroscopic finite element method was used to simulate the multi-pass forging process of TC18 titanium alloy bar, and the macroscopic finite element model coupled with mesoscopic VPSC model was used to calculate the deformation texture. The good fitting between the experiment and simulation results shows that this method has good reliability. Furthermore, the formation and evolution of texture in the forging bar can be predicted. Thus, the process parameters can be adjusted based on the prediction to obtain the alloy bar with the designed production needs. Because many influence factors are not considered in this model, such as phase transformation, recrystallization, and shear stress, the simulation model should be further developed.

3 Conclusions

1) During the forging process, the effective strain in the center of TC18 titanium alloy bar is always higher than that at the edge of alloy bar, due to the large deformation zone in the center of alloy bar. In addition, the deformation in center is more uniform than that at the edge. The shear stress σ_{XY} gradually changes from the negative state in the center to the positive state at the edge. With the forging proceeding, the shear stress σ_{XY} in the center is gradually homogenized. The distributions of effective strain and shear stress σ_{XY} have a great influence on the texture evolution at the center and edge of alloy bar.

2) The {110}<112> and {110}<110> textures are transformed into {111}<110> texture in the center of alloy bar after hexagonal forging. In the center-formed of alloy bar, the {111} and {110} textures are mutually transformed, i.e., the stretching texture <110>//normal direction (ND) of body-centered cubic (bcc) structure can be easily formed by stretching, and the compression textures <100> and <111>// ND of bcc structure can be easily formed by upsetting. The {100} and {111} textures are mainly formed at the edge of alloy bar due to the smaller deformation at the edge.

3) The simulated and measured texture results of three passes show a good fitting result. The prediction for the edge of alloy bar exhibits a little lager deviation than that in the center of alloy bar does, because of the recrystallization of the edge during forging, leading to random textures. The basic characteristics of deformation texture remain after forging. The center texture after forging process is formed by the interaction of hexagonal forging and mutual transformation of {110} and {111} textures, and it is similar to the shear texture. The weak {100} texture and strong {111} texture appear in both the simulation and experiment results, indicating that {100} texture at the edge of forging bar is derived from the deformation process of alloy bar.

4) The <110> and <111> oriented grains are hard-oriented grains, while the <100> oriented grains are soft-oriented grains. Therefore, {110} and {111} textures are expected and the {100} texture is unfavorable in the actual production. The hexagonal forging can barely produce unfavorable {100} texture, and it is conducive to the weakening and elimination of {100} texture. The tensile test results show that all the mechanical properties of the hexagonal forging specimens can meet the standard requirements.

References

1 Liang Houquan, Guo Hongzhen, Ning Yongquan *et al*. *Acta Metallurgica Sinica*[J], 2014, 50(7): 871 (in Chinese)

2 Qiao Enli, Feng Yongqi, Li Weiqing *et al. Metal World*[J], 2013(4): 54 (in Chinese)

3 Lu Kaikai, Duan Qihui, Wang Chengzhang. *World Nonferrous Metals*[J], 2016(8): 63 (in Chinese)

4 Fan X G, Zhang Y S, Zheng H J *et al*. *Materials Characterization*[J], 2018, 137: 151

5 Zhang Yongqiang, Guo Hongzhen, Lei Wenguang *et al*. *Titanium Industry Progress*[J], 2015, 32(2): 17 (in Chinese)

6 Chang L L, Zheng L W. *Transactions of Nonferrous Metals Society of China*[J], 2018, 28(6): 1114

7 Zhang Yongqiang, Guo Hongzhen, Liu Rui *et al*. *Rare Metal Materials and Engineering*[J], 2013, 42(3): 634 (in Chinese)

8 Zhao Yongqing. *Phase Transformation and Heat Treatment of Titanium Alloy*[M]. Changsha: Central South University Press, 2009 (in Chinese)

9 Ma Jimin, He Jinyu, Pang Kechang. *Titanium Ingot and Forging* [M]. Beijing: Metallurgical Industry Press, 2012 (in Chinese)

10 Li Kai, Yang Ping, Sha Aixue *et al*. *Acta Metallurgica Sinica*[J], 2014, 50(6): 707 (in Chinese)

11 Meng L, Kitashima T, Tsuchiyama T *et al*. *Materials Science & Engineering A*[J], 2020, 771: 138 640

12 Meng L, Kitashima T, Tsuchiyama T *et al*. *Metallurgical and Materials Transactions A*[J], 2021, 52(1): 303

13 Sheng J W, Wang Z Y, Zheng L H *et al*. *Journal of the Minerals, Metals and Materials Society*[J], 2019, 71(12): 4687

14 Meng L, Kitashima T, Tsuchiyama T *et al*. *Metallurgical and Materials Transactions A*[J], 2020, 51(11): 5912

15 Zhao J, Dargusch M, Davies C H J. *Proceedings of the 12th World Conference on Titanium*[C]. Beijing: Science Press, 2012: 763

16 Bantounas I, Dye D, Lindley T. *Acta Materialia*[J], 2010, 58(11): 3908

17 Lebensohn R A, Canova G R. *Acta Materialia*[J], 1997, 45(9): 3687

18 Tome C N, Lebensohn R A. *Visco-plastic Self-Consistent*[R]. Los Alamos: Los Alamos National Laboratory, 2009

19 Chen Liquan, Yang Ping, Li Zhishang *et al*. *Rare Metal Materials and Engineering*[J], 2021, 50(10): 3600 (in Chinese)

20 Li Zhishang, Chen Liquan, Yang Ping *et al*. *Journal of Plasticity Engineering*[J], 2021, 28(9): 94 (in Chinese)

大型TC18钛合金棒材多火次锻造过程的织构演变模拟

李志尚[1]，熊智豪[1]，杨　平[1]，顾新福[1]，颜孟奇[2]，沙爱学[2]

(1. 北京科技大学 材料科学与工程学院，北京 100083)

(2. 中国航发北京航空材料研究院，北京 100095)

摘　要：使用了一种多尺度耦合的方法来预测大型TC18钛合金棒材织构。首先采用宏观有限元方法，模拟了TC18钛合金棒材在接近实际工艺条件下的多火次锻造过程，并得出了在锻造过程中棒材芯部与边部的等效应变及剪切应力σ_{XY}分布不均匀的特征。然后，通过宏观有限元模型与介观粘塑性自洽模型（VPSC）多尺度耦合的方法模拟得到了锻造过程中棒材芯部和边部织构的演变情况。结果表明，六方锻造方式使棒材芯部由{110}<112>织构过渡到{111}<110>织构，并由{110}<110>织构过渡到{111}<110>织构。整个锻造过程中即是{111}型织构与{110}型织构相互转变的过程。这种过渡织构在极图中呈现出类似于剪切织构的特点，经分析：这种织构并非是剪切织构，而是锻造过程中由六方锻造方式和{110}、{111}型2类织构间的相互转变共同作用下形成的。经过棒材的形变过程，边部形成了{100}和{111}型2种织构。通过对比发现，六方锻造方式不仅不易生成{100}型织构，而且有利于{100}型织构的减弱和消除。拉伸试验结果表明，六方锻造样品的力学性能均达到标准要求。

关键词：钛合金；多火次锻造；织构；模拟

作者简介：李志尚，男，1996年生，硕士，北京科技大学材料科学与工程学院，北京 100083，E-mail：G20198398@xs.ustb.edu.cn